THE JOURNAL OF PHYSICAL CHEMISTRY A
A JOURNAL OF THE AMERICAN CHEMICAL SOCIETY

pubs.acs.org/JPCA

Article

Disorder in P3HT Nanoparticles Probed by Optical Spectroscopy on P3HT-*b*-PEG Micelles

Patrick Beer, Paul M. Reichstein, Konstantin Schötz, Dominic Raithel, Mukundan Thelakkat, Jürgen Köhler, Fabian Panzer, and Richard Hildner*

Cite This: *J. Phys. Chem. A* 2021, 125, 10165−10173

Read Online

ACCESS | Metrics & More | Article Recommendations | Supporting Information

ABSTRACT: We employ photoluminescence (PL) spectroscopy on individual nanoscale aggregates of the conjugated polymer poly(3-hexylthiophene), P3HT, at room temperature (RT) and at low temperature (LT) (1.5 K), to unravel different levels of structural and electronic disorder within P3HT nanoparticles. The aggregates are prepared by self-assembly of the block copolymer P3HT-*block*-poly(ethylene glycol) (P3HT-*b*-PEG) into micelles, with the P3HT aggregates constituting the micelles' core. Irrespective of temperature, we find from the intensity ratio between the 0−1 and 0−0 peaks in the PL spectra that the P3HT aggregates are of H-type nature, as expected from π-stacked conjugated thiophene backbones. Moreover, the distributions of the PL peak ratios demonstrate a large variation of disorder between micelles (inter-aggregate disorder) and within individual aggregates (intra-aggregate disorder). Upon cooling from RT to LT, the PL spectra red-shift by 550 cm^{-1}, and the energy of the (effective) carbon-bond stretch mode is reduced by 100 cm^{-1}. These spectral changes indicate that the P3HT backbone in the P3HT-*b*-PEG copolymer does not fully planarize before aggregation at RT and that upon cooling, partial planarization occurs. This intra-chain torsional disorder is ultimately responsible for the intra- and inter-aggregate disorder. These findings are supported by temperature-dependent absorption spectra on thin P3HT films. The interplay between intra-chain, intra-aggregate, and inter-aggregate disorder is key for the bulk photophysical properties of nanoparticles based on conjugated polymers, for example, in hierarchical (super-) structures. Ultimately, these properties determine the usefulness of such structures in hybrid organic−inorganic materials, for example, in (bio-)sensing and optoelectronics applications.

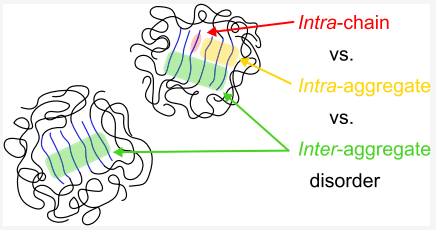

INTRODUCTION

Nanoparticles based on conjugated polymers attract significant attention owing to their potential applications in (bio-)sensing, (bio-)imaging and hybrid organic−inorganic opto-electronics.[1−3] Such nanoparticles can also be used as building blocks for the self-assembly of hierarchical structures with tailored properties, for instance, for efficient hole and electron transporting layers in organic (hybrid) solar cells or for larger functional (super)structures on a meso- and macroscopic scale.[3,4] Interesting properties of nanoparticles emerge upon self-assembly from amphiphilic block copolymers, with one block being a conjugated polymer, like the prototypical poly(3-hexylthiophene), P3HT, and a second block being a polar polymer, such as poly(ethylene glycol) (PEG). While P3HT possesses characteristic semiconducting properties with a band gap of around 2 eV corresponding to the photon energy in the visible spectral range,[5] the PEG block is able to coordinate metallic or inorganic semiconductor nanoparticles.[4] The resulting hybrid nanoparticles are highly interesting for optoelectronic applications.[3,4] Yet, their successful exploitation requires a clear understanding of the electronic and photophysical properties of the (aggregated) conjugated polymer block, which plays a key role for the overall functionality of the nanoparticles.

We study single nanoparticles that are self-assembled from a $P3HT_{68}$-*b*-PEG_{454} block copolymer into nanoscale spherical or oval micelles in aqueous solution (Figure 1a,b). The micelles' core comprises P3HT aggregates with a size of about 25 nm that form via π-stacking of the thiophene backbones; the PEG block forms a disordered corona around the P3HT core.[6] We chose P3HT-based block copolymers because this conjugated polymer is the fruit fly in the field and its photophysical properties, when molecularly dissolved and aggregated, are well established.[7−20] Hence, spectral features can be related to structural and electronic properties of P3HT nanoparticles (here, the micelles' P3HT core). Although nanoparticles and nanofibers self-assembled from P3HT homopolymers were extensively investigated in the past,[21−23] the focus of that previous work was mainly on revealing the interplay of electronic coupling along thiophene backbones (intra-chain) and between π-stacked backbones (inter-chain) within self-

Received: September 23, 2021
Revised: November 8, 2021
Published: November 19, 2021

https://doi.org/10.1021/acs.jpca.1c08377
J. Phys. Chem. A 2021, 125, 10165−10173

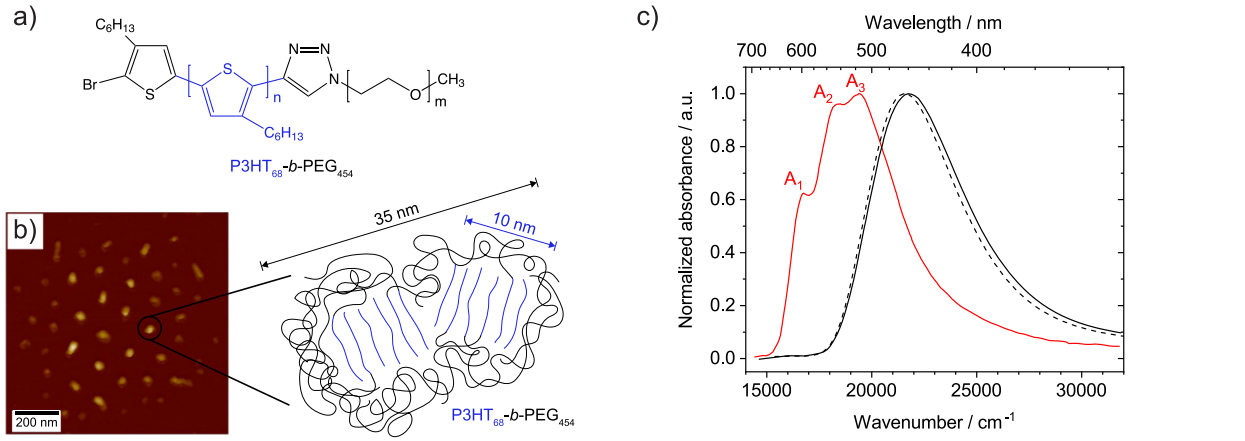

Figure 1. (a) Chemical structure of the P3HT-*b*-PEG block copolymer (n = 68; m = 454). (b) AFM image of P3HT-*b*-PEG micelles formed in aqueous solution (left) with an illustration of the aggregated P3HT core (right, blue) and the disordered PEG corona (black). The AFM image was adapted with permission from ref 6. Copyright 2016 American Chemical Society. (c) UV/vis absorption spectra of the P3HT-*b*-PEG block copolymer and a P3HT homopolymer dissolved in the "good" solvent chloroform (black solid and dashed), as well as of P3HT-*b*-PEG micelles in aqueous solution (red).

assembled nanostructures.[24−30] If intra-chain coupling dominates, the nanostructures are of J-type and feature photoluminescence (PL) spectra that possess a more intense electronic 0−0 peak relative to the 0−1 peak.[24,27,31] In contrast, dominating inter-chain coupling results in H-aggregated nanostructures that show PL spectra with a suppressed 0−0 peak.[24,26,27] By controlling the processing conditions, the molecular weight, polydispersity, and/or regioregularity of P3HT, the ratio between intra- and inter-chain coupling could be changed, resulting in transitions between J-type and H-type behavior.[24,26,27] However, the impact of the different sources of structural, and consequently, electronic disorder on the photophysics of P3HT-based nanostructures has not been studied in detail yet.

Here, we investigate the interplay between intra-chain, intra-aggregate (or inter-chain), and inter-aggregate disorder in nanoscale P3HT aggregates within the core of single P3HT-*block*-PEG (P3HT-*b*-PEG) micelles using PL spectroscopy at room temperature (RT) and at low temperature (LT) (1.5 K), in combination with temperature-dependent absorption spectroscopy on a thin P3HT film. We find that in the micelles' P3HT core, exclusively H-aggregates are formed by torsionally disordered chains within a π-stack. This intra-chain disorder gives rise to substantial intra-aggregate disorder within the micelles' core and inter-aggregate disorder between micelles. The changes of spectral parameters upon cooling are consistent with H-type aggregation and indicate partial planarization of the P3HT backbones, that is, a reduction of (torsional) disorder, at LT.

MATERIALS AND METHODS

The synthesis of the P3HT-*b*-PEG block copolymer involves coupling of P3HT-alkyne and PEG-N_3 blocks, which was described in detail recently.[6] Here, we use the block copolymer with n = 68 repeating units for the P3HT block (M_n = 11.4 kDa, MALDI-ToF; 17.7 kDa, SEC) and m = 454 for the PEG block (Figure 1a). The regioregularity of the P3HT-alkyne precursor was 96%. For the preparation of micelles, P3HT-*b*-PEG was dissolved in tetrahydrofuran (THF), which yielded a clear orange color indicating non-aggregated P3HT chains in solution. Subsequently, methanol (MeOH) was added at a defined rate until a volume ratio MeOH/THF of 9:1 (vol/vol) was obtained, which led to a color change to violet, characteristic of aggregation of P3HT. Since MeOH is a "poor" solvent for the P3HT block, it minimizes contact with MeOH by dense π-stacking, while the PEG block forms a disordered corona around this P3HT core (Figure 1b). To stabilize the micellar structures, a solvent exchange from MeOH/THF to deionized water was performed by dialysis. The final concentration of this aqueous solution was 0.1 mg/mL, which served as stock solution for our optical experiments (see below). The micelles are mostly spherical (sometimes oval) with an average total diameter of 35 nm, as measured by atomic force microscopy (AFM) (Figure 1b). The average diameter of the P3HT core was determined by cryo-TEM to be 26 nm.[6] For further details on the preparation protocol and structural characterization of the micelles, see ref 6.

For PL spectroscopy on (single) micelles, we employed a home-built confocal microscopy setup including a liquid-helium bath cryostat, as described in detail recently.[19,20] Briefly, the micelles were excited at the absorption maximum of the crystalline P3HT core (532 ± 2 nm, Figure 1c) by a super-continuum fiber laser (Fianium SC400, NKT). The excitation light was cleaned up by a bandpass filter (532/10, AHF), was attenuated by a variable optical density filter, passed a spatial filter, and was focused onto the sample by an objective (NA = 0.85, Edmund Optics) that was mounted inside the bath cryostat. To excite the isolated micelles, the excitation beam was scanned across the sample using a motorized scan mirror combined with two telecentric lenses. The PL was collected by the same objective, passed long pass filters, and was focused onto the entrance slit of a spectrograph (Acton SP2150, Princeton Instruments) equipped with a scientific CMOS camera (Zyla 4.2, Andor) or an emCCD camera (iXon, Andor). Measurements as a function of the excitation polarization were performed by flipping a motorized half-wave plate into the excitation path; for all other measurements, a quarter-wave plate was used to excite with circularly polarized light. For spectroscopy of single micelles, we diluted the stock solution 1:300 (vol/vol) in deionized water. About 5 μL of this dilute solution was dropped on a glass substrate (Spectrosil 2000), which was immediately covered by a microscopy cover slip (UQG Optics). This

https://doi.org/10.1021/acs.jpca.1c08377
J. Phys. Chem. A 2021, 125, 10165−10173

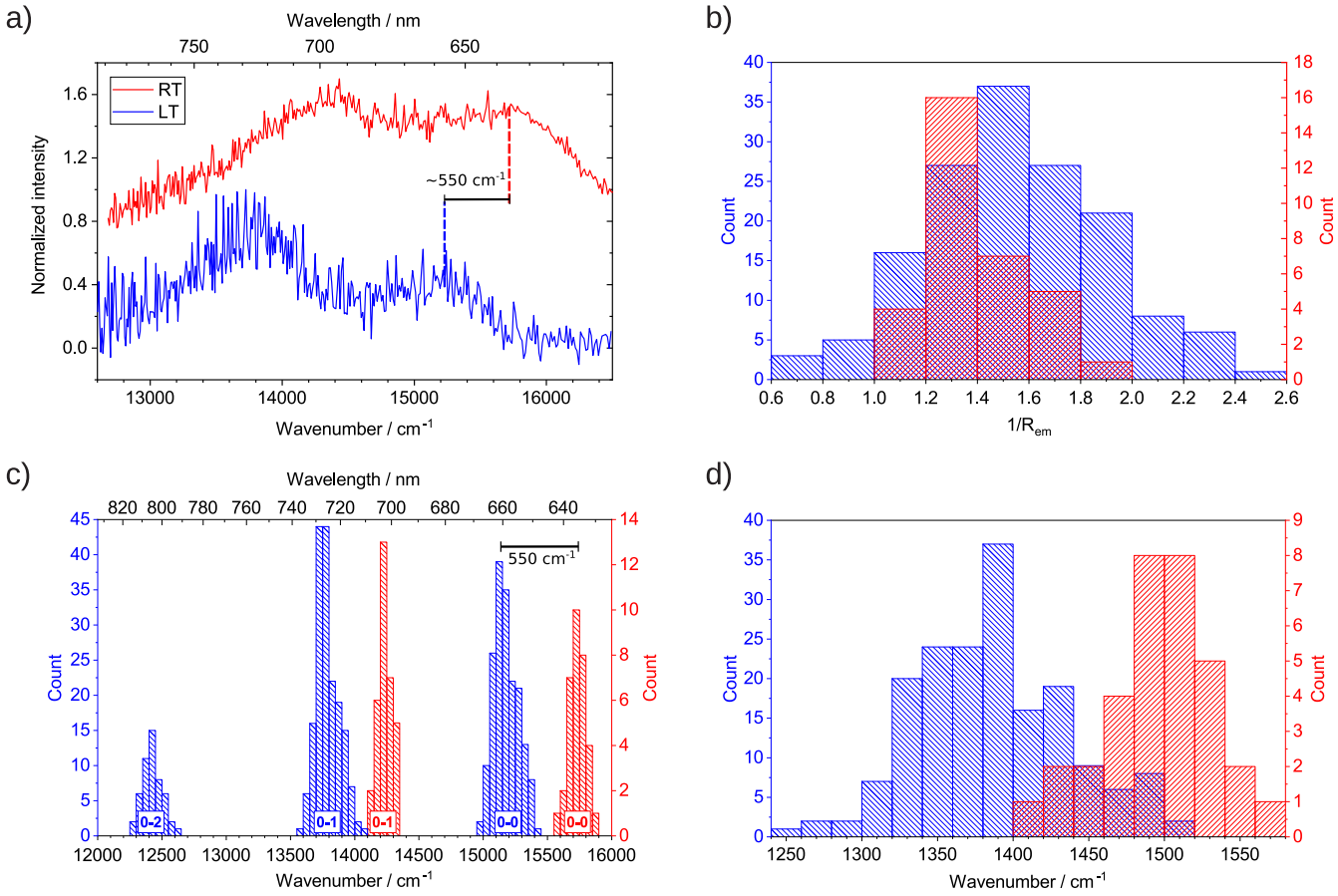

Figure 2. (a) PL spectra of single P3HT-*b*-PEG micelles, cast from aqueous solution on substrates, at RT (red) and at LT (1.5 K, blue). (b) Histogram of the inverse emission peak ratio $1/R_{em} = I_{01}/I_{00}$, with I_{0i} (i = 0,1) being the integrated intensity of the 0−i transition of the PL spectra. (c) Distributions of the 0−i (i = 0,1,2) PL peak positions. (d) Distribution of the vibrational energies, that is, the energy difference between the 0−0 and 0−1 PL peak positions. In (b−d), red bars display data from RT spectra, and the blue bars represent data from LT spectra.

sample was mounted in the cryostat that was purged with helium gas for RT measurements or was cooled to 1.5 K by immersion in liquid helium.

For the preparation of P3HT thin films, regioregular P3HT[15] with a molecular weight of M_n = 7.1 kDa (MALDI-ToF; M_w = 12.5 kDa, SEC) and a polydispersity index of 1.11 was dissolved in THF at a concentration of 2.0 mg/mL. The thin film was spin-coated under ambient conditions at 2000 rpm, after casting 70 μL on a glass substrate. Based on the optical density of the thin film (Supporting Information, Figure S6) and the absorption coefficient of P3HT,[13] the thickness of the film was estimated to be around 20−30 nm.

Temperature-dependent absorption measurements of P3HT thin films were performed in a home-built setup. The sample is placed in a temperature-controlled continuous-flow helium cryostat (Oxford Instruments). A tungsten lamp is used as a white light source for absorption measurements. The transmitted light is detected using a spectrograph (Shamrock SR303i) connected to a CCD-Camera (iDus DU420a-OE, Andor). The temperature-dependent absorption spectra were offset-corrected by subtracting a spectrally constant offset (see Figure S6a for the as-measured absorption spectrum at 300 K).

Fitting of spectra was performed by home-written scripts. PL spectra of micelles were fitted by a sum of two Gaussian functions to retrieve the integrated PL peak intensities and the spectral positions and line widths of the peaks. The fits are weighted by E^3 to account for the energy (E) dependence of the spontaneous emission process. To fit the absorption spectra, we followed the approach put forward by Spano and co-workers and used a modified Franck−Condon progression described in refs 11 and 32

$$I_{Abs}(\hbar\omega) \propto (n\cdot\hbar\omega)\cdot\sum_m \left(\frac{S^m}{m!}e^{-S}\right)\left(1 - \frac{We^{-S}}{2\hbar\omega_m}G_m\right)^2 \cdot\Gamma\cdot\delta(\hbar\omega - (\hbar\omega_0 + m\hbar\omega_m)) \quad (1)$$

with

$$G_m = \frac{\sum_{k\neq m} S^k}{k!(k-m)} \quad (2)$$

Here, n is the refractive index at photon energy h$\hbar\omega$, S is the Huang−Rhys parameter of non-interacting chains, m and k are quantum numbers of the dominant (effective) carbon-bond stretch vibration with energy h$\hbar\omega_m$, h$\hbar\omega_0$ is the energy of the lowest-energy A_1 transition, and W is the free exciton bandwidth. Γ is a Gaussian line shape function with line width σ to account for inhomogeneous line broadening, and δ is the delta-distribution (see Supporting Information, SI, Figures S1 and S6).

RESULTS AND DISCUSSION

Absorption Spectra of Micelles in Solution. Figure 1c shows RT absorption spectra of the dissolved $P3HT_{68}$-*b*-

https://doi.org/10.1021/acs.jpca.1c08377
J. Phys. Chem. A 2021, 125, 10165−10173

PEG_{454} block copolymer (solid black) and, for comparison, of a regioregular (>98%) P3HT homopolymer with 144 repeating units (dashed black). Both spectra were acquired from chloroform solution, a "good" solvent for P3HT. We find nearly identical, broad, and structureless spectra with maxima around 22 000 cm^{-1} (450 nm) that are characteristic for dissolved P3HT with a disordered conformation.[33] The minor spectral blue-shift of the P3HT-*b*-PEG absorption is likely related to the presence of the PEG block. This long and polar PEG block causes a slightly different effective refractive index for the P3HT block in the copolymer and/or might induce more torsional disorder in the P3HT backbone. The absorption spectrum of P3HT-*b*-PEG micelles (Figure 1c, red) in aqueous solution (0.1 mg/mL stock solution), a "poor" solvent for P3HT, is substantially red-shifted with respect to that of P3HT in chloroform, and it features a distorted vibronic progression. This spectral shape is a clear signature of H-aggregation of P3HT[16,23,24,26,29,32,34] with π−stacked thiophene backbones within the micelles' cores. Shoulders/peaks appear at 16 660 cm^{-1} (600 nm), 18 130 cm^{-1} (551 nm), and 19 600 cm^{-1} (510 nm), labeled A_i (i = 1,2,3) with increasing energy, which stem from transitions into delocalized vibronic exciton states characterized by different vibrational quantum numbers n.[11,35] In particular, the lowest-energy (highest-wavelength) transition A_1 into the (n = 0) exciton band has lower intensity with respect to the higher-energy transition A_2 into the (n = 1) exciton band, clearly indicating H-aggregation.[11,35] From a fit with a modified Franck−Condon progression (Materials and Methods, and Figure S1), we obtain a free exciton bandwidth of 710 cm^{-1}, which is in the range previously reported for aggregated P3HT in films and solutions.[8,11,12,16,17,32,34]

PL Spectroscopy of Single Micelles. To gain insights into the interplay of (inter-aggregate, intra-aggregate, and intra-chain) disorder in the P3HT aggregates in the micelles' core, we diluted the stock solution in deionized water (1:300 vol/vol) and performed PL spectroscopy on single micelles (Figure 2). In Figure 2a, we show PL spectra of individual micelles at RT (red) and LT (1.5 K, blue, see also Supporting Information, Figures S2 and S3). At both temperatures, emission occurs below a photon energy of about 16 660 cm^{-1} (above 600 nm) with the LT PL being red-shifted by about 550 cm^{-1}. The double-peak structure of the 0−0 and 0−1 PL peaks with the (slightly) weaker 0−0 peak compared to the 0−1 peak is characteristic for emission of aggregated P3HT.[16,17,32,34] For quantitative analysis, we fitted the PL spectra for in total 33 (RT) and 177 (LT) micelles by a sum of two Gaussian functions and retrieved the integrated PL peak intensities, peak positions, and line widths (Figures 2 and S4).

Inverse Emission Peak Ratio: Intra- and Inter-Aggregate Disorder. The degree of intra-aggregate disorder (within a single micelle's core) and inter-aggregate disorder (between different micelles) is reflected in the distributions of the inverse emission peak ratio $1/R_{em} = I_{01}/I_{00}$ (Figure S5).[16] Here, I_{01} and I_{00} are the integrated intensities of the 0−1 and the 0−0 transitions in the PL spectra. For ideal, disorder-free H-aggregates at T = 0 K, the 0−0 PL transition is entirely forbidden (I_{00} = 0); hence, $1/R_{em} \rightarrow \infty$ since the wavefunction of the emitting exciton features perfect symmetry with alternating phase from chain to chain along the π-stack of an aggregate.[36,37] With increasing intra-aggregate disorder, the relative 0−0 peak intensity I_{00} increases, thus $1/R_{em}$ decreases, until the limit of strong disorder is reached. In this limit, disorder is much larger than the electronic coupling between P3HT chains, and the emitting exciton becomes strongly localized on very few adjacent P3HT chains along a π-stack. The inverse emission peak ratio $1/R_{em}$ of PL spectra of aggregates is then identical to that of isolated, non-interacting chains, which, in turn, is quantified by the Huang−Rhys parameter S. For the analysis of the PL spectra in this present work, this implies, on the one hand, that the inverse emission peak ratio determined from the PL spectrum of a single micelle is a direct measure for (structural and electronic) intra-aggregate disorder of its H-aggregated P3HT core. On the other hand, if inter-aggregate disorder is present, the PL spectrum of each micelle will yield a specific $1/R_{em}$ value, characteristic of the specific degree of disorder in its core. The width of the distribution of $1/R_{em}$ values from PL spectra of different micelles thus provides a measure for inter-aggregate disorder (Figure S5).

The histograms of the inverse emission peak ratios determined from the RT and LT spectra are shown in Figure 2b as red and blue bars, respectively. The distributions of $1/R_{em}$ range from 1.0 to 2.0 (RT) and 0.6 to 2.6 (LT). The smaller width of the RT histogram may be related to the smaller number of investigated micelles. Nevertheless, both distributions are rather broad and thus indicate a strong variation of disorder from micelle to micelle, that is, a large inter-aggregate disorder, independent of temperature.

Generally, for all PL spectra at RT and for most PL spectra at LT, we find $1/R_{em} > 1$. For those micelles, the 0−1 PL peak dominates in the PL spectrum as expected for H-aggregated P3HT. Yet, each P3HT core still features substantial intra-aggregate disorder since the 0−0 PL peak is not entirely suppressed in the spectra of single micelles. In the LT histogram, we find a few $1/R_{em}$ values as small as 0.6, that is, the PL spectra of those micelles possess a dominating 0−0 PL peak. This latter shape of the PL spectra is often associated with *J*-aggregate behavior in P3HT-based nanofibers and nanoparticles.[24,26,30,31] We note, however, that those small inverse emission peak ratios are essentially identical to the Huang−Rhys parameter of S = 0.7 for isolated, non-interacting P3HT chains with disordered conformation that we recently determined by single-molecule PL spectroscopy.[20] In other words, for *J*-type behavior, $1/R_{em}$ values must be clearly below 0.7. Therefore, we attribute the LT PL spectra with $1/R_{em} < 1$ to originate from H-aggregated P3HT cores of micelles with a very high degree of intra-aggregate disorder. In this situation, the emitting excitons are strongly localized on very few adjacent P3HT chains along a π-stack of the aggregate (Figure S5). This disorder-induced localization of emitting excitons results in "single-chain-like" shapes of PL spectra with a dominating 0−0 PL peak and $1/R_{em} \approx S$. We recently observed a similar behavior in H-type nanostructures based on a small organic molecule, in which 'monomer-like'-like PL spectra resulted from emitting excitons localized on only ∼2 adjacent molecules.[38]

We suggest that the large degree of inter- and intra-aggregate disorder in the micelles' cores both at RT and LT, evident from the distributions in Figure 2b, has its origin in the sub-structure of the P3HT core. From scattering experiments on P3HT nanofibers, nanoparticles, and semi-crystalline films, it is known that those systems comprise differently oriented crystallites with a size of 6−9 nm in the π-stacking direction (*b*-axis), about 8−25 nm along the direction defined by the conjugated P3HT backbone (*c*-axis), and 8−13 nm along the

https://doi.org/10.1021/acs.jpca.1c08377
J. Phys. Chem. A 2021, 125, 10165−10173

"alkyl-side-chain" direction (*a*-axis).[22,23,28,31,39] The P3HT core of our micelles with a size of ∼25 nm might thus comprise several crystallites along the π-stacking direction with different relative orientations (given the contour length of the P3HT block of about 26 nm, along the *c*-axis largely extended chain crystallites are formed,[40] see also Figure 1b, right, and Supporting Information, Figure S2). Since the disorder can vary between crystallites within the core of a single micelle and between the cores of different micelles, the large intra- and inter-aggregate disorder observed here is reasonable.

PL Peak Positions: Intra-Chain Torsional Disorder. Figure 2c displays the histograms of PL peak positions with red (blue) bars, representing the RT (LT) data. For 51 out of the 177 investigated micelles at LT, the signal-to-background ratio was high enough to determine the position of the 0−2 PL peak as well. At RT, the PL peak positions are distributed around 15 733 cm^{-1} (635 nm) for the 0−0 transition and around 14 237 cm^{-1} (702 nm) for the 0−1 transition. At LT, the 0−0 PL peak positions are spread around 15 178 cm^{-1} (659 nm), the 0−1 positions around 13 791 cm^{-1} (725 nm), and the 0−2 positions around 12 426 cm^{-1} (805 nm). The average spectral red-shift when going from RT to LT is thus about 550 cm^{-1}. All distributions of peak positions are relatively narrow with standard deviations between 50 and 96 cm^{-1}. Since the emission stems from the lowest-energy vibronic exciton states, those data indicate that the energy position of the emitting states (relative to the ground state) is rather well defined for our system without much inter-aggregate variation.

The positions and (temperature-dependent) red-shift of the PL spectra of the P3HT-*b*-PEG micelles follow the general trend found in the literature for P3HT aggregates.[7,11,12,16,24,31,34] The precise numbers, however, depend on the aggregate formation of P3HT, which in turn depends sensitively on the sample and preparation conditions (molecular weight, polydispersity, regioregularity, solvent, concentration, temperature window, and rate of temperature change during preparation, etc.[12,16,17,24,31,34]). At RT, the mean spectral position of the 0−0 PL peaks of the micelles is similar to that found for (single) P3HT nanofibers,[24,31] but it is blue-shifted by more than 500 cm^{-1} with respect to the 0−0 PL peak of (semi-crystalline) P3HT films[16,34] and of P3HT aggregates in solution.[12] Especially, in films of conjugated polymers, energy transfer toward lower-energy emitting excitons can lead to more red-shifted PL.[9,12,41−43] However, given typical exciton diffusion lengths of around 8 nm for P3HT[44,45] and diameters of the P3HT cores of our micelles of ∼25 nm, energy transfer cannot contribute substantially to spectral differences between micelles and bulk films. We thus attribute the spectral difference between films/solutions and micelles to a higher degree of (structural and electronic) intra-aggregate disorder in the P3HT core of the P3HT-*b*-PEG micelles compared to the disorder in the crystallites in films. Owing to the long PEG block with 454 repeating units, steric effects in the micelles' disordered PEG corona can introduce strain into the P3HT core, which prevents P3HT chains to pack in a more ordered fashion. The P3HT block within the copolymer does not fully planarize before assembly into π-stacks, and some remaining intra-chain torsional disorder of the thiophene backbone prevails[9,24] in the aggregated micelles' core (see also the discussion below). Intra-chain torsional disorder shifts transition (site) energies of non-interacting chains to higher energies.[20,46−48] Consequently, emitting exciton states at the bottom of the exciton band in aggregates with torsionally disordered constituent building blocks are blue-shifted as well. Since there are many different realizations of intra-chain torsional disorder, which give rise to broad site energy distributions,[19,46,47] this results ultimately in structural and electronic intra-aggregate and inter-aggregate disorder.

Having established that the micelles' cores are formed by torsionally disordered P3HT chains, we now discuss the origin of the spectral red-shift of the micelles' PL by on average 550 cm^{-1} upon cooling from RT to LT (Figure 2c). A combination of several effects plays a role for this spectral shift (Figure 3):

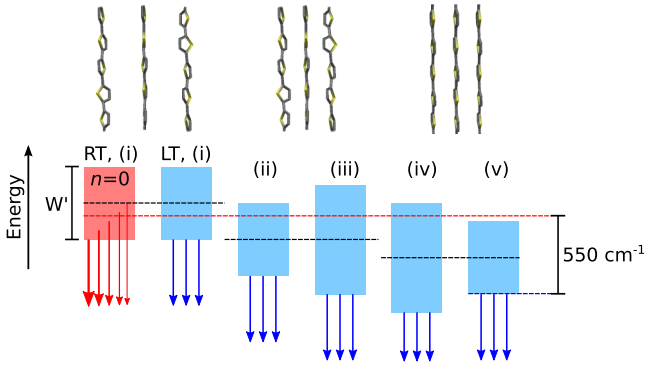

Figure 3. Illustration of the contributions to the exciton bandwidth of the lowest-energy (n = 0) exciton band and the energy position of the emitting exciton states of P3HT aggregates upon cooling from RT to LT. (i) P3HT aggregates are assembled from torsionally disordered chains (top). At RT, emission (solid arrows) stems from thermally populated exciton states within the (n = 0) exciton band (red), whereas this thermal population is frozen out at LT (blue), and emission comes only from the bottom state(s). (ii,iii) Cooling reduces the distance between chains (top). This increases non-resonant dispersion interactions between P3HT chains, which shifts the entire exciton band to lower energies without changing the bandwidth (ii); this smaller distance additionally increases electronic interactions between P3HT chains, which widens the exciton band but does not shift its center energy (iii). (iv,v) Chain planarization toward LT (top). This decreases site energies of P3HT chains, which further shifts the exciton band to lower energies (iv); at the same time, planarization delocalizes intra-chain excitations along chains, which decreases electronic coupling (exciton bandwidth) due to the H-type nature of P3HT aggregates (v). Black dashed horizontal lines indicate the corresponding center energies of the exciton band, and the red and blue dashed lines mark the (average) energy of the emitting exciton at RT and LT, respectively. The exciton bandwidth W' is related to the free exciton bandwidth W via $W' = We^{-S}$, with S being the Huang−Rhys parameter of non-interacting chains.[11] Absorption occurs into the top state of the exciton bands.

(i) At RT, emission does not only stem from the lowest-energy exciton state but also from thermally populated higher-energy vibronic exciton states within the lowest-energy (n = 0) vibronic exciton band. Cooling to 1.5 K freezes out this thermal population of higher-energy exciton states, which accounts for a red-shift of about 200 cm^{-1},[16] corresponding to the change in available thermal energy. (ii) Thermal compression of the P3HT core of micelles upon cooling reduces inter-chain distances and increases non-resonant dispersion interactions between P3HT chains. These interactions typically shift transition (site) energies to lower energies, accounting for a red-shift of about 200−250 cm^{-1} of the entire exciton band and thus of the emitting exciton states, as estimated by Spano et al.[16] (iii) A further consequence of decreasing inter-chain distances between

https://doi.org/10.1021/acs.jpca.1c08377
J. Phys. Chem. A 2021, 125, 10165−10173

P3HT backbones toward LT is an increasing electronic coupling between P3HT chains. Hence, the exciton band width becomes wider, which further shifts the emitting exciton states at the bottom of the $n = 0$ band down in energy. (iv) Torsionally disordered P3HT chains within the aggregates in the micelles' cores (partially) planarize upon cooling.[24] For non-interacting P3HT chains, planarization enhances intra-chain delocalization of electronic excitations and shifts transition energies toward lower energies (Figure S5).[19,46] Consequently, in aggregates with more planar chains, the emitting exciton states are shifted to lower energies as well. (v) Finally, for increasingly planar conjugated polymer chains with stronger intra-chain delocalization, the inter-chain electronic coupling decreases due to the H-type nature of the aggregates.[16,49,50] This reduces the exciton bandwidth and blue-shifts the emitting exciton states. Taken together, effects (i) and (ii) account for 400−450 cm^{-1} of the total spectral red-shift of the micelles' PL spectra of 550 cm^{-1} upon cooling. The red-shifting effects (iii) and (iv) compete with the blue-shifting contribution (v) to account for the remaining temperature-dependent red-shift of 100−150 cm^{-1}. To resolve this competition, we performed temperature-dependent absorption spectroscopy.

Temperature-Dependent Absorption of P3HT Films. Since absorption measurements on films of micelles were not possible due to strong scattering setting in toward LT, we recorded temperature-dependent absorption spectra from P3HT films with a thickness of about 20−30 nm, corresponding to the size of our micelles' P3HT core (see the materials and methods section). The absorption spectra of the P3HT thin film at RT (Figure 4, red) and LT (5 K, blue)

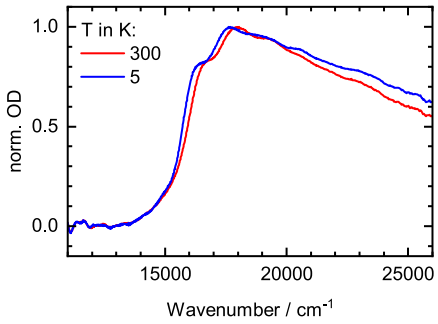

Figure 4. Normalized absorption spectra of a thin P3HT film at RT (300 K, red) and LT (5 K, blue).

demonstrate its semi-crystalline nature with aggregates of π-stacked chains coexisting with disordered (amorphous) regions;[32,34] for the full set of temperature-dependent absorption spectra, see Supporting Information, Figure S6. The spectral shape matches qualitatively that of the absorption spectrum of the micelles in aqueous solution (Figure 1c). Accordingly, we analyzed the film absorption spectra using a modified Frank-Condon analysis (see the materials and methods section and Figure S6). We find that the A_i (i = 1,2,3) transitions are located at 16 640, 18 075, and 19 510 cm^{-1} at RT. Upon cooling, the absorption spectrum shifts to lower energies by 230 cm^{-1}. Furthermore, we find the free exciton bandwidth to be 200 cm^{-1} independent of temperature, also being reflected in the constant A_1/A_2 peak ratio, as shown in Figure 4. While the free exciton bandwidth is still in the range of values reported for P3HT,[8,11,12,16,17,32,34] it is smaller than the value determined for the micelles in aqueous solution (Figures 1c and S1). Consequently, the inter-chain electronic coupling must be smaller in the film as well. This reduced coupling can be traced back to the smaller degree of intra-chain torsional disorder of P3HT chains in films, for which inter-chain electronic coupling is reduced due to the H-type nature of P3HT aggregates, in agreement with the discussion above.

Returning to the discussion related to the different contributions that impact the free exciton bandwidth upon cooling, the film data clearly show a constant bandwidth independent of temperature. Hence, all effects impacting on the bandwidth cancel each other out [effects (iii) and (v) above]. Assuming that the exciton bandwidth does not change much for the P3HT aggregates in the micelles' core, a similar cancellation of effects takes place and the position of the emitting excitons at the bottom of the lowest-energy exciton band cannot be influenced (much) by contributions (iii) and (v) either. The only remaining factor is thus contribution (iv), the red-shift in transition (site) energies due to planarization (increased intra-chain delocalization) upon cooling, to account for the remaining 100−150 cm^{-1} red-shift of the PL of the micelles.

We emphasize that the chain planarization in the micelles' core upon cooling is only a small effect. First, even at RT, the P3HT backbones must be nearly planar since they are densely packed into aggregates with a reasonably high free exciton bandwidth (Figure 1c). Moreover, in our recent work, we studied the transition from a torsionally disordered P3HT chain, with an average dihedral angle between thiophene units of 145°, to a fully planarized chain with a dihedral angle of 180° (without inter-chain electronic coupling).[19,20] Based on time-dependent density functional theory calculations, we estimated that this full planarization gives rise to a spectral red-shift of up to 4800 cm^{-1}.[19] Hence, the corresponding red-shift of 100−150 cm^{-1} reported here can only result from a very small change in dihedral angles.

Vibrational Energies: Chain Planarization upon Cooling. Finally, a further independent piece of evidence for the presence of torsionally disordered P3HT chains within the aggregated cores of micelles and for chain planarization upon cooling comes from the energies of vibrational modes coupling to electronic transitions. From the energy difference between the 0−0 and 0−1 peaks in the PL spectra of single micelles, we find that at RT, the distribution of vibrational energies is spread around a mean value of 1496 cm^{-1}, and at LT, it is distributed around 1387 cm^{-1} (Figure 2d). The widths of those distributions are 36 cm^{-1} (RT) and 50 cm^{-1} (LT), respectively. Although both vibrational energies are in agreement with (aromatic) carbon-bond stretch modes found for conjugated polymers,[12,16,51] the average shift of about 100 cm^{-1} upon cooling is nevertheless surprising and has, to the best of our knowledge, never been reported for P3HT. To understand this shift, it is important to keep in mind that the 0−1 transition in bulk samples (which includes the P3HT core in our micelles) is an effective transition that results from a superposition of several individual vibronic lines in the range from 1300 cm^{-1} to about 1600 cm^{-1}, as seen in LT single-chain PL spectra.[10,19,20] These individual lines cannot be resolved in bulk samples due to the usually broad spectral lines (Figure S3). The relative intensities and spectral positions of individual vibronic lines are known to be very sensitive to conformational changes of conjugated polymer chains and lead

https://doi.org/10.1021/acs.jpca.1c08377
J. Phys. Chem. A 2021, 125, 10165−10173

to the well-known "missing-mode effect" observed, for example, for poly(phenylenevinylene) derivatives.[52] In that work, a change in the effective vibrational frequency of about 100 cm^{-1} was attributed to a substantial intensity change in a low-energy individual vibronic transition, induced by chain planarization.[52]

For P3HT, a combination of intensity and vibrational energy changes of individual transitions is likely to be responsible for the shift of the effective vibrational energy in the aggregated micelles' cores upon cooling: first, the totally symmetric and strong Я mode, an aromatic C═C vibration,[53−57] shifts from ∼1470 cm^{-1} for a non-aggregated (torsionally disordered) chain to ∼1450 cm^{-1} in an aggregate[51,55,56] (comprising torsionally less disordered chains). Second, the combined C═C and C−C mode at the hexyl connection of the backbone at ∼1380 cm^{-1} gains intensity upon planarization.[51,56] Finally, at 1624 cm^{-1}, a stretching mode associated with a quinoidal structure of the P3HT backbone was identified.[58] Since excited states in torsionally disordered P3HT possess charge-transfer character,[20,48] which implies some degree of quinoidal character, this 1624 cm^{-1} mode may be relevant in torsionally disordered chains. Yet, this mode is suppressed by chain planarization when the charge-transfer character of excited states of thiophenes is substantially reduced.[20] The combination of those (intensity and energy) changes of individual vibronic transitions will shift the energy of the effective vibrational mode to lower energy. This shift in the energy of the effective vibrational mode supports our notion of planarization of P3HT chains in the core of the micelles upon cooling from RT to LT. Ultimately, aggregation of P3HT with intra-chain torsional disorder contributes to the intra-aggregate (and inter-aggregate) disorder in the micelles' cores that we identified above using the inverse emission peak ratio.

CONCLUSIONS

In summary, we resolved a hierarchy of different levels of structural and electronic disorder in P3HT nanoparticles by investigating PL spectra from isolated micelles based on a P3HT-*b*-PEG block copolymer with an aggregated P3HT core. We found a strong variation of the shape of the PL spectra that we analyzed in terms of the inverse emission peak ratio $1/R_{em} = I_{01}/I_{00}$, that is, the intensity ratio of the 0−1 and 0−0 PL peaks. This ratio is broadly distributed, suggesting a large variation of disorder from micelle to micelle (inter-aggregate disorder). The values of $1/R_{em}$ are <2 and can be as small as 0.6. For this range, the relative 0−0 PL peak intensity of the P3HT aggregates is smaller compared with the situation in non-aggregated chains; yet, the 0−0 PL peak is not completely suppressed. Hence, those $1/R_{em}$ data are a clear signature of H-aggregation of P3HT within the micelles' core, but with substantial intra-aggregate disorder. The red-shift of the PL spectra observed upon cooling from RT to LT (1.5 K) allowed us to conclude that this inter-aggregate and intra-aggregate disorder comes from aggregation of P3HT chains with torsionally disordered backbones, that is, with intra-chain disorder. Upon cooling, a partial planarization occurs, which shifts the emitting excitons in P3HT aggregates to lower energies. This notion was supported by a temperature-dependent shift of the vibrational energy, the energy difference between the 0−0 and 0−1 PL peaks, and by temperature-dependent absorption spectroscopy of a thin P3HT film. Torsional (structural) disorder implies electronic disorder since the transition (site) energy of each P3HT chain depends on the specific realization of torsional disorder. The resulting distribution of site energies translates into aggregates with electronic intra-aggregate and inter-aggregate disorder. Our data thus allowed us to disentangle inter-aggregate, intra-aggregate, and intra-chain (structural and electronic) disorder within H-type P3HT aggregates. Understanding this interplay of disorder is, in combination with electronic interactions between polymer chains, important to fully characterize the photophysics of nanoparticles and ultimately determines their potential applicability in opto- and bio-electronic devices.

ASSOCIATED CONTENT

Supporting Information

The Supporting Information is available free of charge at https://pubs.acs.org/doi/10.1021/acs.jpca.1c08377.

Modified Franck−Condon analysis of absorption spectra of micelles in aqueous solutions and of a thin P3HT film; polarization-dependent PL spectroscopy, scanning confocal imaging of micelles; and line widths of vibronic transitions in PL spectra (PDF)

AUTHOR INFORMATION

Corresponding Author

Richard Hildner − *Spectroscopy of Soft Matter, University of Bayreuth, 95440 Bayreuth, Germany; Zernike Institute for Advanced Materials, University of Groningen, 9747 AG Groningen, The Netherlands;* orcid.org/0000-0002-7282-3730; Email: r.m.hildner@rug.nl

Authors

Patrick Beer − *Spectroscopy of Soft Matter, University of Bayreuth, 95440 Bayreuth, Germany*

Paul M. Reichstein − *Applied Functional Polymers, University of Bayreuth, 95440 Bayreuth, Germany*

Konstantin Schötz − *Soft Matter Optoelectronics, University of Bayreuth, 95440 Bayreuth, Germany*

Dominic Raithel − *Spectroscopy of Soft Matter, University of Bayreuth, 95440 Bayreuth, Germany*

Mukundan Thelakkat − *Applied Functional Polymers, Bavarian Polymer Institute, and Bayreuther Institut für Makromolekülforschung (BIMF), University of Bayreuth, 95440 Bayreuth, Germany;* orcid.org/0000-0001-8675-1398

Jürgen Köhler − *Spectroscopy of Soft Matter, Bavarian Polymer Institute, and Bayreuther Institut für Makromolekülforschung (BIMF), University of Bayreuth, 95440 Bayreuth, Germany;* orcid.org/0000-0002-4214-4008

Fabian Panzer − *Soft Matter Optoelectronics, University of Bayreuth, 95440 Bayreuth, Germany;* orcid.org/0000-0002-2191-9011

Complete contact information is available at: https://pubs.acs.org/10.1021/acs.jpca.1c08377

Notes

The authors declare no competing financial interest.

ACKNOWLEDGMENTS

This work was financially supported by the German Research Foundation DFG within project GRK1640 (K.S., D.R., J.K., M.T., and R.H.) and the Bavarian State Ministry of Science,

Research and the Arts within the collaborative research network Solar Technologies Go Hybrid (J.K. and M.T.).

REFERENCES

(1) Persson, N. E.; Chu, P.-H.; McBride, M.; Grover, M.; Reichmanis, E. Nucleation, Growth, and Alignment of Poly(3-Hexylthiophene) Nanofibers for High-Performance OFETs. *Acc. Chem. Res.* **2017**, *50*, 932−942.
(2) Jin, X.-H.; Price, M. B.; Finnegan, J. R.; Boott, C. E.; Richter, J. M.; Rao, A.; Menke, S. M.; Friend, R. H.; Whittell, G. R.; Manners, I. Long-Range Exciton Transport in Conjugated Polymer Nanofibers Prepared by Seeded Growth. *Science* **2018**, *360*, 897−900.
(3) MacFarlane, L. R.; Shaikh, H.; Garcia-Hernandez, J. D.; Vespa, M.; Fukui, T.; Manners, I. Functional Nanoparticles through π-Conjugated Polymer Self-Assembly. *Nat. Rev. Mater.* **2021**, *6*, 7−26.
(4) Lin, Y.; Daga, V. K.; Anderson, E. R.; Gido, S. P.; Watkins, J. J. Nanoparticle-Driven Assembly of Block Copolymers: A Simple Route to Ordered Hybrid Materials. *J. Am. Chem. Soc.* **2011**, *133*, 6513−6516.
(5) Chatterjee, S.; Jinnai, S.; Ie, Y. Nonfullerene Acceptors for P3HT-Based Organic Solar Cells. *J. Mater. Chem. A* **2021**, *9*, 18857−18886.
(6) Reichstein, P. M.; Gödrich, S.; Papastavrou, G.; Thelakkat, M. Influence of Composition of Amphiphilic Double-Crystalline P3HT-b-PEG Block Copolymers on Structure Formation in Aqueous Solution. *Macromolecules* **2016**, *49*, 5484−5493.
(7) Brown, P. J.; Thomas, D. S.; Köhler, A.; Wilson, J. S.; Kim, J.; Ramsdale, C. M.; Sirringhaus, H.; Friend, R. H. Effect of Interchain Interactions on the Absorption and Emission of Poly(3-Hexylthiophene). *Phys. Rev. B: Condens. Matter Mater. Phys.* **2003**, *67*, 064203.
(8) Scharsich, C.; Lohwasser, R. H.; Sommer, M.; Asawapirom, U.; Scherf, U.; Thelakkat, M.; Neher, D.; Köhler, A. Control of Aggregate Formation in Poly(3-Hexylthiophene) by Solvent, Molecular Weight, and Synthetic Method. *J. Polym. Sci. B Polym. Phys.* **2012**, *50*, 442−453.
(9) Parkinson, P.; Müller, C.; Stingelin, N.; Johnston, M. B.; Herz, L. M. Role of Ultrafast Torsional Relaxation in the Emission from Polythiophene Aggregates. *J. Phys. Chem. Lett.* **2010**, *1*, 2788−2792.
(10) Thiessen, A.; Vogelsang, J.; Adachi, T.; Steiner, F.; Vanden Bout, D.; Lupton, J. M. Unraveling the Chromophoric Disorder of Poly(3-Hexylthiophene). *Proc. Natl. Acad. Sci. U.S.A.* **2013**, *110*, E3550−E3556.
(11) Spano, F. C. Modeling Disorder in Polymer Aggregates: The Optical Spectroscopy of Regioregular Poly(3-Hexylthiophene) Thin Films. *J. Chem. Phys.* **2005**, *122*, 234701.
(12) Panzer, F.; Sommer, M.; Bässler, H.; Thelakkat, M.; Köhler, A. Spectroscopic Signature of Two Distinct H-Aggregate Species in Poly(3-Hexylthiophene). *Macromolecules* **2015**, *48*, 1543−1553.
(13) Theander, M.; Inganäs, O.; Mammo, W.; Olinga, T.; Svensson, M.; Andersson, M. R. Photophysics of Substituted Polythiophenes. *J. Phys. Chem. B* **1999**, *103*, 7771−7780.
(14) Shen, X.; Hu, W.; Russell, T. P. Measuring the Degree of Crystallinity in Semicrystalline Regioregular Poly(3-Hexylthiophene). *Macromolecules* **2016**, *49*, 4501−4509.
(15) Panzer, F.; Bässler, H.; Lohwasser, R.; Thelakkat, M.; Köhler, A. The Impact of Polydispersity and Molecular Weight on the Order-Disorder Transition in Poly(3-Hexylthiophene). *J. Phys. Chem. Lett.* **2014**, *5*, 2742−2747.
(16) Spano, F. C.; Clark, J.; Silva, C.; Friend, R. H. Determining Exciton Coherence from the Photoluminescence Spectral Line Shape in Poly(3-Hexylthiophene) Thin Films. *J. Chem. Phys.* **2009**, *130*, 074904.
(17) Reichenberger, M.; Baderschneider, S.; Kroh, D.; Grauf, S.; Köhler, J.; Hildner, R.; Köhler, A. Watching Paint Dry: The Impact of Diiodooctane on the Kinetics of Aggregate Formation in Thin Films of Poly(3-Hexylthiophene). *Macromolecules* **2016**, *49*, 6420−6430.
(18) Grégoire, P.; Vella, E.; Dyson, M.; Bazán, C. M.; Leonelli, R.; Stingelin, N.; Stavrinou, P. N.; Bittner, E. R.; Silva, C. Excitonic Coupling Dominates the Homogeneous Photoluminescence Excitation Linewidth in Semicrystalline Polymeric Semiconductors. *Phys. Rev. B: Condens. Matter Mater. Phys.* **2017**, *95*, 180201.
(19) Raithel, D.; Baderschneider, S.; de Queiroz, T. B.; Lohwasser, R.; Köhler, J.; Thelakkat, M.; Kümmel, S.; Hildner, R. Emitting Species of Poly(3-Hexylthiophene): From Single, Isolated Chains to Bulk. *Macromolecules* **2016**, *49*, 9553−9560.
(20) Raithel, D.; Simine, L.; Pickel, S.; Schötz, K.; Panzer, F.; Baderschneider, S.; Schiefer, D.; Lohwasser, R.; Köhler, J.; Thelakkat, M.; et al. Direct Observation of Backbone Planarization via Side-Chain Alignment in Single Bulky-Substituted Polythiophenes. *Proc. Natl. Acad. Sci. U.S.A.* **2018**, *115*, 2699−2704.
(21) Ihn, K. J.; Moulton, J.; Smith, P. Whiskers of Poly(3-Alkylthiophene)s. *J. Polym. Sci. B Polym. Phys.* **1993**, *31*, 735−742.
(22) Roehling, J. D.; Arslan, I.; Moulé, A. J. Controlling Microstructure in Poly(3-Hexylthiophene) Nanofibers. *J. Mater. Chem.* **2012**, *22*, 2498−2506.
(23) Oosterbaan, W. D.; Vrindts, V.; Berson, S.; Guillerez, S.; Douhéret, O.; Ruttens, B.; D'Haen, J.; Adriaensens, P.; Manca, J.; Lutsen, L.; et al. Efficient Formation, Isolation and Characterization of Poly(3-Alkylthiophene) Nanofibres: Probing Order as a Function of Side-Chain Length. *J. Mater. Chem.* **2009**, *19*, 5424−5435.
(24) Niles, E. T.; Roehling, J. D.; Yamagata, H.; Wise, A. J.; Spano, F. C.; Moulé, A. J.; Grey, J. K. J-Aggregate Behavior in Poly-3-Hexylthiophene Nanofibers. *J. Phys. Chem. Lett.* **2012**, *3*, 259−263.
(25) Baghgar, M.; Labastide, J.; Bokel, F.; Dujovne, I.; McKenna, A.; Barnes, A. M.; Pentzer, E.; Emrick, T.; Hayward, R.; Barnes, M. D. Probing Inter- and Intrachain Exciton Coupling in Isolated Poly(3-Hexylthiophene) Nanofibers: Effect of Solvation and Regioregularity. *J. Phys. Chem. Lett.* **2012**, *3*, 1674−1679.
(26) Baghgar, M.; Labastide, J. A.; Bokel, F.; Hayward, R. C.; Barnes, M. D. Effect of Polymer Chain Folding on the Transition from H- to J-Aggregate Behavior in P3HT Nanofibers. *J. Phys. Chem. C* **2014**, *118*, 2229−2235.
(27) Labastide, J. A.; Baghgar, M.; McKenna, A.; Barnes, M. D. Time- and Polarization-Resolved Photoluminescence Decay from Isolated Polythiophene (P3HT) Nanofibers. *J. Phys. Chem. C* **2012**, *116*, 23803−23811.
(28) Labastide, J. A.; Baghgar, M.; Dujovne, I.; Venkatraman, B. H.; Ramsdell, D. C.; Venkataraman, D.; Barnes, M. D. Time- and Polarization-Resolved Photoluminescence of Individual Semicrystalline Polythiophene (P3HT) Nanoparticles. *J. Phys. Chem. Lett.* **2011**, *2*, 2089−2093.
(29) Nagarjuna, G.; Baghgar, M.; Labastide, J. A.; Algaier, D. D.; Barnes, M. D.; Venkataraman, D. Tuning Aggregation of Poly-(3-Hexylthiophene) within Nanoparticles. *ACS Nano* **2012**, *6*, 10750−10758.
(30) Baghgar, M.; Pentzer, E.; Wise, A. J.; Labastide, J. A.; Emrick, T.; Barnes, M. D. Cross-Linked Functionalized Poly(3-Hexylthiophene) Nanofibers with Tunable Excitonic Coupling. *ACS Nano* **2013**, *7*, 8917−8923.
(31) Martin, T. P.; Wise, A. J.; Busby, E.; Gao, J.; Roehling, J. D.; Ford, M. J.; Larsen, D. S.; Moulé, A. J.; Grey, J. K. Packing Dependent Electronic Coupling in Single Poly(3-Hexylthiophene) H- and J-Aggregate Nanofibers. *J. Phys. Chem. B* **2012**, *117*, 4478−4487.
(32) Clark, J.; Chang, J.-F.; Spano, F. C.; Friend, R. H.; Silva, C. Determining Exciton Bandwidth and Film Microstructure in Polythiophene Films Using Linear Absorption Spectroscopy. *Appl. Phys. Lett.* **2009**, *94*, 163306.
(33) Panzer, F.; Bässler, H.; Köhler, A. Temperature Induced Order−Disorder Transition in Solutions of Conjugated Polymers Probed by Optical Spectroscopy. *J. Phys. Chem. Lett.* **2016**, *8*, 114−125.
(34) Clark, J.; Silva, C.; Friend, R. H.; Spano, F. C. Role of Intermolecular Coupling in the Photophysics of Disordered Organic Semiconductors: Aggregate Emission in Regioregular Polythiophene. *Phys. Rev. Lett.* **2007**, *98*, 206406.

https://doi.org/10.1021/acs.jpca.1c08377
J. Phys. Chem. A 2021, 125, 10165−10173

(35) Spano, F. C.; Silva, C. H- and J-Aggregate Behavior in Polymeric Semiconductors. *Annu. Rev. Phys. Chem.* **2014**, *65*, 477−500.
(36) Spano, F. C. The Spectral Signatures of Frenkel Polarons in H- and J-Aggregates. *Acc. Chem. Res.* **2010**, *43*, 429−439.
(37) Kreger, K.; Schmidt, H.-W.; Hildner, R. Tailoring the Excited-State Energy Landscape in Supramolecular Nanostructures. *Electron. Struct.* **2021**, *3*, 023001.
(38) Wittmann, B.; Wenzel, F. A.; Wiesneth, S.; Haedler, A. T.; Drechsler, M.; Kreger, K.; Köhler, J.; Meijer, E. W.; Schmidt, H.-W.; Hildner, R. Enhancing Long-Range Energy Transport in Supramolecular Architectures by Tailoring Coherence Properties. *J. Am. Chem. Soc.* **2020**, *142*, 8323−8330.
(39) Brinkmann, M. Structure and Morphology Control in Thin Films of Regioregular Poly(3-Hexylthiophene). *J. Polym. Sci. B Polym. Phys.* **2011**, *49*, 1218−1233.
(40) Wu, Z.; Petzold, A.; Henze, T.; Thurn-Albrecht, T.; Lohwasser, R. H.; Sommer, M.; Thelakkat, M. Temperature and Molecular Weight Dependent Hierarchical Equilibrium Structures in Semiconducting Poly(3-Hexylthiophene). *Macromolecules* **2010**, *43*, 4646−4653.
(41) Kersting, R.; Lemmer, U.; Mahrt, R. F.; Leo, K.; Kurz, H.; Bässler, H.; Göbel, E. O. Femtosecond Energy Relaxation in π-Conjugated Polymers. *Phys. Rev. Lett.* **1993**, *70*, 3820−3823.
(42) Hildner, R.; Lemmer, U.; Scherf, U.; Köhler, J. Picosecond Excitation Energy Relaxation Processes in a Ladder-Type π-Conjugated Polymer. *Chem. Phys. Lett.* **2006**, *429*, 103−108.
(43) Westenhoff, S.; Beenken, W. J. D.; Friend, R. H.; Greenham, N. C.; Yartsev, A.; Sundström, V. Anomalous Energy Transfer Dynamics Due to Torsional Relaxation in a Conjugated Polymer. *Phys. Rev. Lett.* **2006**, *97*, 166804.
(44) Shaw, P. E.; Ruseckas, A.; Samuel, I. D. W. Exciton Diffusion Measurements in Poly(3-Hexylthiophene). *Adv. Mater.* **2008**, *20*, 3516−3520.
(45) Goh, C.; Scully, S. R.; McGehee, M. D. Effects of Molecular Interface Modification in Hybrid Organic-Inorganic Photovoltaic Cells. *J. Appl. Phys.* **2007**, *101*, 114503.
(46) Barford, W.; Bittner, E. R.; Ward, A. Exciton Dynamics in Disordered Poly(p-Phenylenevinylene). 2. Exciton Diffusion. *J. Phys. Chem. A* **2012**, *116*, 10319−10327.
(47) Barford, W. Excitons in Conjugated Polymers: A Tale of Two Particles. *J. Phys. Chem. A* **2013**, *117*, 2665−2671.
(48) Simine, L.; Rossky, P. J. Relating Chromophoric and Structural Disorder in Conjugated Polymers. *J. Phys. Chem. Lett.* **2017**, *8*, 1752−1756.
(49) Wiesenhofer, H.; Beljonne, D.; Scholes, G. D.; Hennebicq, E.; Brédas, J.-L.; Zojer, E. Limitations of the Förster Description of Singlet Exciton Migration: The Illustrative Example of Energy Transfer to Ketonic Defects in Ladder-Type Poly(Para-Phenylenes). *Adv. Funct. Mater.* **2005**, *15*, 155−160.
(50) Gierschner, J.; Huang, Y. S.; Van Averbeke, B.; Cornil, J.; Friend, R. H.; Beljonne, D. Excitonic versus Electronic Couplings in Molecular Assemblies: The Importance of Non-Nearest Neighbor Interactions. *J. Chem. Phys.* **2009**, *130*, 044501.
(51) Gao, Y.; Grey, J. K. Resonance Chemical Imaging of Polythiophene / Fullerene Photovoltaic Thin Films : Mapping Morphology-Dependent Aggregated and Unaggregated C = C Species. *J. Am. Chem. Soc.* **2009**, *131*, 9654−9662.
(52) Wise, A.; Grey, J. Understanding the Structural Evolution of Single Conjugated Polymer Chain Conformers. *Polymers* **2016**, *8*, 388.
(53) Donohoo-Vallett, P. J.; Bragg, A. E. π-Delocalization and the Vibrational Spectroscopy of Conjugated Materials: Computational Insights on Raman Frequency Dispersion in Thiophene, Furan, and Pyrrole Oligomers. *J. Phys. Chem. B* **2015**, *119*, 3583−3594.
(54) Louarn, G.; Trznadel, M.; Buisson, J. P.; Laska, J.; Pron, A.; Lapkowski, M.; Lefrant, S. Raman Spectroscopic Studies of Regioregular Poly(3-Alkylthiophenes). *J. Phys. Chem.* **1996**, *100*, 12532−12539.
(55) Milani, A.; Brambilla, L.; Del Zoppo, M.; Zerbi, G. Raman Dispersion and Intermolecular Interactions in Unsubstituted Thiophene Oligomers. *J. Phys. Chem. B* **2007**, *111*, 1271−1276.
(56) Brambilla, L.; Tommasini, M.; Botiz, I.; Rahimi, K.; Agumba, J. O.; Stingelin, N.; Zerbi, G. Regio-Regular Oligo and Poly(3-Hexyl Thiophene): Precise Structural Markers from the Vibrational Spectra of Oligomer Single Crystals. *Macromolecules* **2014**, *47*, 6730−6739.
(57) Navarrete, J. T. L.; Zerbi, G. Lattice Dynamics and Vibrational Spectra of Polythiophene. I: Oligomers and Polymer. *J. Chem. Phys.* **1991**, *94*, 957−964.
(58) Baibarac, M.; Lapkowski, M.; Pron, A.; Lefrant, S.; Baltog, I. SERS Spectra of Poly(3-Hexylthiophene) in Oxidized and Unoxidized States. *J. Raman Spectrosc.* **1998**, *29*, 825−832.

https://doi.org/10.1021/acs.jpca.1c08377
J. Phys. Chem. A 2021, 125, 10165−10173